5th Edition

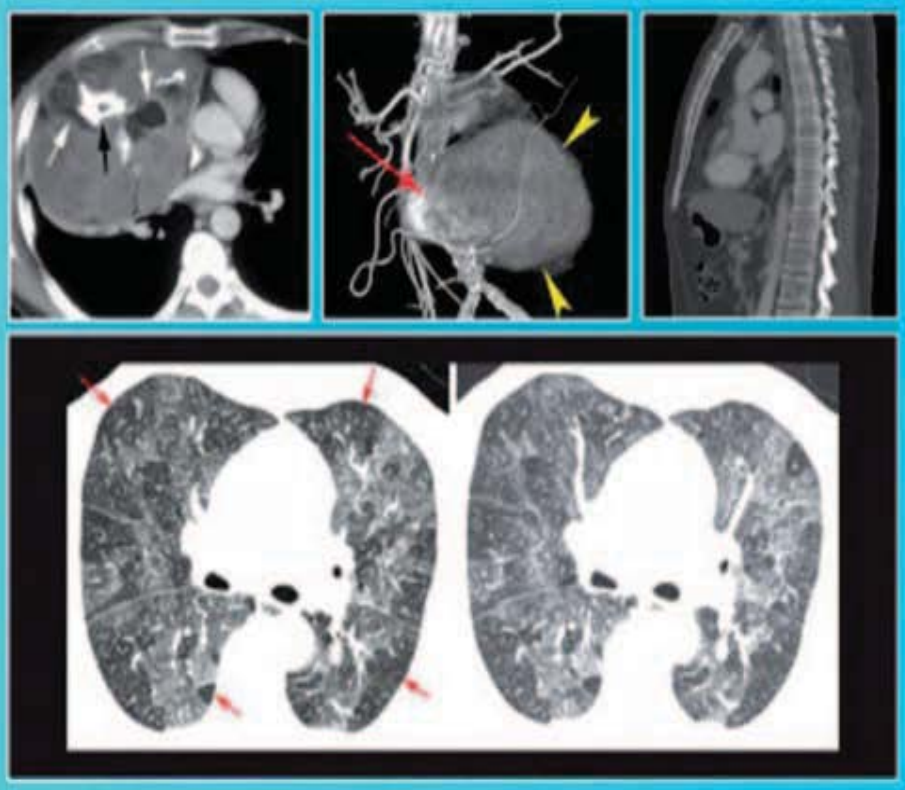

FUNDAMENTALS OF BODY CT

W. RICHARD WEBB
WILLIAM E. BRANT
NANCY M. MAJOR

ELSEVIER

FUNDAMENTALS OF RADIOLOGY SERIES

Fundamentals of Body CT

FIFTH EDITION

W. RICHARD WEBB, MD
Professor Emeritus of Radiology and Biomedical Imaging
Emeritus Member, Haile Debas Academy of Medical Educators
University of California, San Francisco
San Francisco, California

WILLIAM E. BRANT, MD, FACR
Professor Emeritus
Department of Radiology and Medical Imaging
University of Virginia Health System
Charlottesville, Virginia

NANCY M. MAJOR, MD
Professor of Radiology and Orthopedics
University of Colorado School of Medicine
Aurora, Colorado

ELSEVIER

ELSEVIER

3251 Riverport Lane
St. Louis, Missouri 63043

FUNDAMENTALS OF BODY CT, FIFTH EDITION ISBN: 978-0-323-60832-9

Notices

Practitioners and researchers must always rely on their own experience and knowledge in evaluating and using any information, methods, compounds or experiments described herein. Because of rapid advances in the medical sciences, in particular, independent verification of diagnoses and drug dosages should be made. To the fullest extent of the law, no responsibility is assumed by Elsevier, authors, editors or contributors for any injury and/or damage to persons or property as a matter of products liability, negligence or otherwise, or from any use or operation of any methods, products, instructions, or ideas contained in the material herein.

Library of Congress Control Number: 2018964895

Content Strategist: Russell Gabbedy
Content Development Specialist: Angie Breckon
Content Development Manager: Kathryn DeFrancesco
Publishing Services Manager: Shereen Jameel
Senior Project Manager: Umarani Natarajan
Design Direction: Bridget Hoette

Printed in the United States of America

Last digit is the print number: 9 8 7 6 5 4 3 2 1

To Teddy, my grandson
A new addition for the new edition.

W.R.W.

To my wife and true companion, Barbara.
In memory of my daughter, Rachel.
To our children and their spouses and our ten grandchildren: Evan, Finley, Sophia, Katie, Josie, Danielle, Dylan, Grayson, Amelia, and Noah.

W.E.B.

To Kenneth, were it not for you, so much would not be possible…thank you.

N.M.

Preface

Despite the fact that we concentrate on "fundamentals" in this book (that has always been our goal), the fundamentals keep changing and evolving, along with advances in CT techniques, our improved understanding of diseases, and changes in medical practice and disease evaluation. This new edition gives us the chance to update important topics and add new material, including a number of high-quality, state-of-the-art images.

In the chest section, this includes updates in the classification of adenocarcinoma, lung cancer screening (using lung reporting and data system; Lung-RADS), lung cancer staging, and classification and diagnosis of interstitial lung diseases using high-resolution CT.

Additions to the abdominal section include a review of the liver imaging reporting and data system (Li-RADS) for imaging and reporting small hepatocellular carcinoma, and reviews of the Atlanta classification of acute pancreatitis, the revised classification of cystic neoplasms of the pancreas, and an improved description of CT findings of histologic subtypes of renal cell carcinoma.

In the musculoskeletal (MSK) section, an emphasis has been placed on the diagnosis of abnormalities, often incidental, detected on chest and abdominal CT scans obtained for non-MSK indications.

The half-dozen or so years since the third edition was published have seen continued advances in helical CT techniques. In this edition, we review the various spiral/helical CT protocols currently used in clinical practice for the diagnosis of chest, abdominal, and musculoskeletal abnormalities, including discussions of high-resolution CT, lung nodule assessment and lung cancer screening, CT pulmonary embolism diagnosis, CT enterography, CT enteroclysis, CT colonography, and optimizing CT techniques in musculoskeletal diagnosis.

New topics, discussions of additonal diseases (too numerous to mention here), and new images have been added to all chapters, including updated descriptions and illustrations of normal anatomy and incidental findings. Disease classifications, including those for pulmonary adenocarcinoma, diffuse lung diseases, and pancreatic lesions, have been updated where appropriate.

We hope you enjoy and profit from our efforts.

W. Richard Webb
William E. Brant
Nancy M. Major

Contents

CHAPTER 1

Introduction to CT of the Thorax: Chest CT Techniques

W. RICHARD WEBB

Spiral (helical) computed tomography (CT) allows the entire chest to be imaged in a few seconds or less (i.e., during a single breath hold), with volumetric acquisition of scan data. Two- and three-dimensional reformations may be performed if desired. Because scanning is rapid, contrast agents can be injected quickly, excellent vascular opacification can be achieved, and reduced volumes of contrast agent can be used.

Multidetector CT (MDCT) scanners have multiple parallel rows of X-ray detectors (an ever-increasing number, now exceeding 250 in some scanners, and capable of reconstructing more than 500 slices at a time). With MDCT, each of the detector rows records data independently as the gantry rotates; consequently, a volume of the patient (e.g., up to 16 cm along the longitudinal axis, or *z*-axis, with a 256-detector scanner) is imaged with each gantry rotation. With large-area detector scanners, scanning of a volume may be performed without table motion; this is most useful for cardiac imaging. The gantry rotation time is 0.5 seconds or less.

SPIRAL CHEST CT: GENERAL PRINCIPLES

The specific protocols used for chest CT depend on the scanner used, the scanner manufacturer, and the reason for the study. However, several general principles apply to all chest scans (Table 1.1).

Scan Levels

Chest CT is usually performed from a level just above the lung apices (near the suprasternal notch) to the level of the posterior costophrenic angles; these scans also encompass the diaphragm and the upper abdomen. The distance (or volume) needed to cover the thorax (usually 25–30 cm) is determined by a preliminary projection scan (e.g., a "scout view").

Patient Position

Routinely, patients are scanned supine. Prone scans may be obtained for high-resolution CT (HRCT) or to assess movement of pleural fluid collections. The patient may also be positioned prone for biopsy of posterior lung lesions or drainage of pleural fluid collections.

Lung Volume

Scans are routinely obtained after a full inspiration (i.e., at total lung capacity) and during suspended respiration. Postexpiratory scans may be performed in some cases (particularly on HRCT) to assess air trapping.

Detector Row and Slice Thickness

Scan data are usually acquired with the thinnest detector width available on the scanner (detector rows on most scanners range from 0.25 to 0.625 mm), and the reconstructed slice thickness used for scan interpretation is determined by the indication for the scan. For example, if data are recorded with 0.625-mm detectors, slices can be reconstructed at any thickness from 0.625 to 5 mm for viewing. Thin slices are required for some specific indications, whereas thicker slices are quicker to interpret and do not occupy as much memory when they are stored.

Most chest scans are reconstructed with a 1- to 1.25-mm thickness. When one is viewing a study reconstructed with 2.5- or 5-mm-thick slices, if the scan data were collected using thinner detectors, and if the scan data are still available (they are usually preserved on the scanner disk for a day or two), you can have thinner slices reconstructed at a later time.

Usually slices are reconstructed at an interval equal to the slice thickness (e.g., 1.25 mm) to provide a volumetric data set. On occasion, scans are reconstructed at overlapping levels (e.g., 1.25-mm slices reconstructed at 0.625-mm intervals), although this is not generally necessary.

TABLE 1.1
Chest CT: General Principles

Scan levels: Lung apices to the posterior costophrenic angles
Patient position: Supine; prone scans sometimes used for diagnosis of lung disease of pleural effusions
Lung volume: Full inspiration, single breath hold; expiratory scans sometimes used to diagnose air trapping or bronchial abnormalities
Gantry rotation time 0.5 seconds or less in most instances
Scan duration: 2.5 seconds or less for the thorax, with use of multiple-detector CT and fast scanning
Detector width: Usually the thinnest detectors (e.g., 0.625 mm or less) for image acquisition
Pitch (table excursion): Depends on tolerable image noise; increased if noise is OK; decreased if there is a desire for high resolution
Reconstruction algorithm: High-resolution algorithm used for most studies; standard or soft-tissue algorithm usually used for vascular studies
Two- or three-dimensional reconstructions: Not routine; occasionally useful for lung, airway, or vascular studies
Contrast agents: Intravenous contrast agent injection in some cases; oral contrast agents only for gastrointestinal abnormalities

Pitch (Table Excursion)

The term *pitch* refers to the distance the table travels during a complete gantry rotation divided by the width of all the detectors used (e.g., table excursion/detector width × number of detector rows). With MDCT, pitch usually ranges from 1 to 2. The higher the pitch, the faster the scan, but images are generally noisier, spatial resolution is reduced somewhat, and the effective slice thickness (the thickness of the patient that is actually imaged) is increased.

Keep in mind that with the spiral technique the actual thickness of the slice you view (i.e., "effective slice thickness") may be greater than the slice thickness you select (e.g., 1.25 mm), depending on the pitch or table excursion during gantry rotation; the greater the pitch, the greater the effective slice thickness. Thus there is a trade-off; with a higher pitch, the study is quicker but the scans are not quite as good.

Scan Duration

MDCT of the chest can be easily performed during a single breath hold (2.5 seconds or less), generally avoiding respiratory motion artifacts, except in very dyspneic or uncooperative patients.

Reconstruction Algorithm

Once the scans have been performed, the scan data are reconstructed using an algorithm that determines some characteristics of the resulting image. For routine chest imaging, a *high-resolution algorithm* is often used to optimize detail, but this makes the image somewhat noisy in appearance. A standard or *soft-tissue algorithm*, which produces a smoother image, is better for assessing thoracic vascular structures (e.g., studies performed for diagnosis of pulmonary embolism, aneurysm, or aortic dissection) but is not optimal for other chest imaging. This algorithm is often used for abdominal imaging.

Two- and Three-Dimensional Reconstruction

Because the scan data are acquired continuously and volumetrically by spiral CT, scans may be reconstructed in any plane desired. A variety of display techniques have been used for imaging the thorax. These include multiplanar reconstructions, three-dimensional shaded surface display or volume rendering from an external perspective, or shaded surface or volume rendering from an internal (i.e., endoluminal) perspective, also known as *virtual bronchoscopy*.

Multiplanar, two-dimensional reconstructions offer the advantage of being quickly performed and are sufficient for diagnosis in most cases in which a reformation is considered desirable. Subsequent chapters provide a number of examples of two-dimensional reconstructions. Three-dimensional techniques, such as shaded surface display and volume rendering, can be valuable in selected cases, but they are time-consuming and require operator experience. These techniques are not commonly used in day-to-day clinical chest imaging.

Maximum- or minimum-intensity projection images representing a slab of three-dimensional data reconstructed from a volumetric data set may sometimes be useful in imaging pulmonary, airway, or vascular abnormalities.

Window Settings

For chest CT, scans must be viewed with at least three different window settings. Scans are usually viewed with a workstation having preset windows available. The presets used when one is reading chest CT scans are generally termed *lung*, *soft-tissue* (or *mediastinal*), and *bone* windows, names that also describe their primary use. These preset windows are often adjusted by the viewer during scan interpretation to optimize visibility of certain structures or abnormalities of interest.

Lung windows typically have a window mean of approximately -600 to -700 Hounsfield units (HU) and a window width of 1000 to 1500 HU. Lung windows best demonstrate lung anatomy and disease, contrasting soft-tissue structures with surrounding air-filled lung parenchyma.

Mediastinal or *soft-tissue windows* (window mean 20–40 HU; window width 450–500 HU) demonstrate soft-tissue anatomy in the mediastinum and in other areas of the thorax, allowing the differentiation of fat, fluid, tissue, calcium, and contrast-opacified vessels. This window is also of value in providing information about consolidated lung, the hila, pleural disease, and structures of the chest wall. Subsequent chapters discuss more specific uses of these two windows. In the assessment of vascular structures (e.g., for pulmonary embolism or dissection diagnosis), a wider window or higher window mean than that used for a routine mediastinal window is often selected by the radiologist to better see detail within the dense contrast column.

Bone windows typically have a window mean of approximately 300 to 500 HU and a window width of 2000 HU. They best demonstrate skeletal structures or very dense objects. This window is sometimes valuable in looking at densely opacified vascular structures.

SPIRAL CHEST CT: PROTOCOLS

In most patients, chest CT is performed with a routine protocol. This technique is designed to provide useful information about the lung, mediastinum, hila, pleura, and chest wall. It is valuable in the diagnosis of a variety of diseases and types of abnormalities. Modified CT techniques are used in specific clinical settings or to look for specific abnormalities (e.g., pulmonary embolism, aortic dissection, and diffuse lung disease). Subsequent chapters provide detailed reviews of some specific protocols.

With current scanners having a large number of detector rows (e.g., 128), protocols for evaluation of different types of thoracic abnormalities have become similar, because scanning with thin slices and with excellent contrast opacification can easily be obtained during a single breath hold regardless of why the scan is being done. A general understanding of the principles involved in obtaining CT scans for specific indications is much more important than knowing detailed specific protocols because these differ with different scanners and manufacturers, and among different institutions.

Use of Contrast Agents

Chest CT can be performed with or without the administration of an intravenous contrast agent, depending on the indication for the study. Scans obtained to rule out pulmonary metastases or to assess lung disease, generally do not require the use of contrast agent. Contrast agent should be used in patients with suspected hilar, mediastinal, or pleural abnormalities and in patients with possible vascular abnormalities. If you are unsure of the indication for the scan, the use of a contrast agent is generally appropriate.

With MDCT, injection of contrast agent at 3 to 5 mL per second, 10 to 30 seconds before scanning begins and for the duration of the scan series, provides excellent opacification of vascular structures. For routine indications, injection of contrast agent at 3 mL per second is generally sufficient. When a vascular abnormality is suspected, injection at 5 mL per second is usually used. The rate of contrast agent injection and the scan delay (the time between the start of contrast agent injection and the start of scanning) differ depending on the reason for the study.

Scanning is begun when the vessels of interest are opacified. For pulmonary embolism diagnosis, the pulmonary arteries need to be opacified; this usually requires a 10- to 15-second delay, although timing the scan to the aorta or left atrium may be beneficial. For diagnosis of aortic abnormalities, a delay of usually 20 to 30 seconds is needed. The delay differs in individual patients according to a number of factors. Timing the scan delay is usually done with a timing bolus or software available on the scanner, which shows vascular opacification during the injection, and begins scanning when contrast agent appears in the target vessel. The use of an oral contrast agent for opacification of the esophagus and gastrointestinal tract is not necessary unless a specific gastrointestinal (i.e., esophageal) abnormality is suspected.

Routine Chest CT

With an MDCT scanner, I routinely scan the chest with 0.625-mm detectors, with reconstruction of 1.25-mm slices at 1.25-mm intervals. This allows the entire thorax to be scanned in 2.5 seconds or less. Depending on the indication for the study, a high-resolution algorithm or smooth algorithm may be chosen for image reconstruction, and intravenous or oral contrast agents may be used (see earlier). Generally speaking, with the exception of vascular imaging protocols, a high-resolution reconstruction algorithm will be chosen for reconstruction of most chest CT studies. This routine protocol is used for evaluation in most patients not

being assessed for a specific vascular abnormality, such as pulmonary embolism or possible aortic disease, or in patients being evaluated for a diffuse lung disease, which would require a high-resolution CT protocol.

Vascular Imaging Protocols

In some patients, chest CT is performed primarily for the diagnosis of a vascular abnormality suspected on the basis of clinical symptoms or radiographic findings. Common thoracic vascular abnormalities assessed with CT include pulmonary embolism, aortic dissection or aneurysm, and traumatic aortic rupture. Although the protocols for each indication differ among institutions and with different scanners, some general principles apply.

Vascular protocols attempt to optimize the degree of contrast enhancement of the vessels of interest and image resolution, while keeping the length of breath hold and the amount of contrast agent injected at a reasonable value. In general, a relatively smooth reconstruction algorithm is preferred for vascular imaging. Reduced image noise with smooth reconstruction makes it easier to see small filling defects (i.e., pulmonary emboli) and subtle differences in contrast enhancement.

Pulmonary Embolism

For the diagnosis of pulmonary embolism by MDCT, slices 1.25 mm thick at 1.25-mm intervals are sufficient for diagnosis, although scanning is usually performed with the thinnest detectors available (e.g., 0.625 mm). A smooth reconstruction algorithm is generally used. Intravenous contrast agent is injected rapidly (e.g., 5 mL per second). Scanning is begun when the scanner shows the pulmonary arteries or left atrium to be opacified. The delay between the start of contrast agent injection and scanning differs, but it averages about 10 to 15 seconds if pulmonary artery opacification is desired and is somewhat longer for opacification of the left atrium. In large patients, scan noise may make interpretation difficult. In such patients, reconstructing slices 2.5 mm thick may reduce noise and increase accuracy.

Aortic Disease

Aortic abnormalities assessed by CT include dissection, aneurysm, intramural hematoma, penetrating ulcer, and traumatic aortic rupture. A scan series through the thorax with relatively thick (2.5- or 5-mm) slices often precedes contrast agent injection (to look for a high-attenuation intramural hematoma; see Chapter 3). If only the thoracic aorta is being examined, scans through the thorax may be obtained with a protocol similar to that used for pulmonary embolism diagnosis (1.25-mm slices reconstructed at 1.25-mm intervals). Intravenous contrast agent is injected rapidly (e.g., 5 mL per second), and scanning is begun when the scanner shows the left atrium or aorta to be opacified. The scan delay may range from 15 to 30 seconds, depending on the patient. If imaging of the abdominal aorta is also required (e.g., for aortic dissection), scans continue through the abdomen. Quiet breathing during the abdominal portion of the scan is usually allowed if the patient cannot hold his or her breath for the duration of the study.

High-Resolution Lung CT

HRCT is used to diagnose diffuse lung diseases, emphysema, bronchiectasis, and some focal lung lesions (e.g., a solitary nodule). HRCT requires thin slices (e.g., 0.625–1.25 mm) and image reconstruction with a sharp (high-resolution) algorithm, which reduces image smoothing and increases spatial resolution. Although use of a sharp algorithm also increases image noise, this is not usually a problem in the interpretation of lung images. Injection of contrast agent is not necessary for HRCT but may be used on occasion if pulmonary embolism is also a consideration.

Scans performed with the patient supine and prone, and following expiration, are often obtained, at least for the patient's initial examination. *Prone scans* are used to detect subtle posterior lung abnormalities; *expiratory scans* are used to detect air trapping because of airway obstruction.

HRCT can be performed in three different ways:

- *Spaced axial imaging.* Thin slices (e.g., 0.625–1.25 mm) are performed at spaced intervals (e.g., 1–2 cm) without table movement to optimize spatial resolution. Because of the spaced images, the radiation dose is reduced.
- *Volumetric HRCT* using the spiral technique, thin detectors, and 1- to 1.25-mm slice thickness reconstruction. This results in an increased radiation dose and slightly decreased resolution, but the entire thorax is imaged and two- or three-dimensional reconstruction and assessment of other abnormalities (e.g., pulmonary embolism) is also possible. If desired, the scans can be reconstructed with both a high-resolution algorithm (for diagnosis of lung abnormalities) and a smooth algorithm (for diagnosis of vascular abnormalities).
- *Combined volumetric and axial imaging.* In some patients, volumetric imaging is obtained for supine scans, with spaced axial imaging for prone and expiratory images. This optimizes the volume imaged, but with a reduced radiation dose.

Dynamic CT Techniques

The term *dynamic CT* means that a number of scans are performed in sequence. Because spiral scanning is continuous, it is a dynamic technique, but dynamic scanning can also be performed without a spiral technique (i.e., without table and patient motion during the acquisition of scans). Dynamic scanning may be performed at a single level during expiration to detect air trapping or to assess tracheal or bronchial collapse in patients with tracheomalacia or airway disease. Dynamic scanning may also be performed to assess some vascular abnormalities.

Low-Dose CT

Reducing the radiation dose is desirable whenever possible, but generally results in decreased image quality because of increased noise. The term *low-dose CT* usually implies the use of a reduced tube current (milliamperes) during the scan. Low-dose chest CT is usually used in children, for screening of patients (i.e., lung cancer screening), or if multiple follow-up examinations will be necessary in a given patient.

With current MDCT scanners, the tube current can be varied or *modulated* at different levels as the patient is scanned on the basis of the chest wall thickness or amount of soft tissue within the volume being scanned. Because the lungs are not very dense, not as much radiation is needed when the lungs (instead of the shoulders or liver) are being scanned. This technique can significantly reduce the tube current and patient dose, without much loss in scan quality, and is usually used for routine studies. A fixed, higher tube current is sometimes used when high resolution and detail is needed. *Iterative reconstruction* is another technique commonly used to reduce the radiation dose.

RADIATION DOSE WITH CHEST CT

Although the patient risk from radiation exposure during diagnostic CT is small and difficult to determine, medical radiation does result in a finite risk. In clinical practice the patient's potential benefits from a CT study need to be balanced against the small radiation risk. In general, if the study has well-defined clinical utility, it is indicated. Nonetheless, it is important for the radiologist to reduce radiation exposure during diagnostic CT, as long as important diagnostic information is not compromised as a result.

Radiation dose and the associated risk to the patient can be calculated by different methods and measurements, none of which are ideal or necessarily predictive of outcome. The calculation most typically used is effective dose (measured in sieverts or more typically millisieverts), which is determined by summing the absorbed doses to individual organs weighted for their radiation sensitivity. However, because an accurate measurement of all organ doses is difficult to obtain during a clinical examination, as are the risk coefficients specific to age, sex, and the organ being irradiated, the estimated dose is calculated for an idealized 70-kg, 30-year-old patient. Although limited in accuracy and predictive value, the effective dose expressed in millisieverts is the most widely used method for quantification of the radiation dose and comparison of radiologic procedures. Approximate doses for background radiation and thoracic imaging procedures are listed in Table 1.2.

TABLE 1.2
Radiation Dose for Chest CT Protocols

	Radiation Dose (mSv)
Normal yearly background radiation	2.5–3.2
Chest radiograph (single view)	0.05
Routine chest CT (300 mA)	5–7
Routine chest CT (modulated tube current approximately 100–150 mA)	1.5–2
High-resolution CT with volumetric imaging (supine, expiratory; modulated tube current of approximately 100–150 mA)	1.5–2
High-resolution CT with spaced axial images (supine, prone, expiratory)	1
Low-dose volumetric CT (40 mA)	<0.5–1

SUGGESTED READING

Bankier, A. A., & Tack, D. (2010). Dose reduction strategies for thoracic multidetector computed tomography: Background, current Issues, and recommendations. *Journal of Thoracic Imaging, 25*, 278–288.

Boiselle, P. M., Hurwitz, L. M., Mayo, J. R., et al. (2011). Expert opinion: Radiation dose management in cardiopulmonary imaging. *Journal of Thoracic Imaging, 26*, 3.

Lawler, L. P., & Fishman, E. K. (2001). Multi-detector row CT of thoracic disease with emphasis on 3D volume rendering and CT angiography. *Radiographics, 21*, 1257–1273.

Lee, C. H., Goo, J. M., Lee, H. J., et al. (2008). Radiation dose modulation techniques in the multidetector CT era: From basics to practice. *Radiographics, 28*, 1451–1459.

Mayo, J. R. (2009). CT evaluation of diffuse infiltrative lung disease: Dose considerations and optimal technique. *Journal of Thoracic Imaging, 24*, 252–259.

CHAPTER 2

Mediastinum: Introduction and Normal Anatomy

W. RICHARD WEBB

Computed tomography (CT) is commonly used in patients suspected of having a mediastinal mass or vascular abnormality (e.g., an aortic aneurysm). In general, CT is performed in two situations.

First, in patients with a mediastinal abnormality visible on plain radiographs, CT is almost always the preferred imaging procedure. CT is used to confirm the presence of a significant lesion, determine its location and relationship to vascular or nonvascular structures, and characterize the mass as solid, cystic, vascular, enhancing, calcified, inhomogeneous, or fatty.

Second, CT is often used in patients in whom there is clinical suspicion of mediastinal disease, regardless of plain radiograph findings. As an example, patients with lung cancer often have mediastinal lymph node enlargement (i.e., metastases) visible on CT when chest radiographs are normal.

NORMAL MEDIASTINAL ANATOMY

The *mediastinum* is the compartment situated between the lungs, marginated on each side by the mediastinal pleura, anteriorly by the sternum and chest wall, and posteriorly by the spine and chest wall. It contains the heart, great vessels, trachea, esophagus, thymus, considerable fat, and a number of lymph nodes. Many of these structures can be reliably identified on CT by their location, appearance, and attenuation.

For the purpose of CT interpretation, the mediastinum can be thought of as consisting of three almost equal divisions along the longitudinal axis of the patient, the first beginning at the thoracic inlet and the third ending at the diaphragm. In adults, each of these divisions is about 7 to 8 cm long and is thus made up of about 15 contiguous 5-mm slices. These can be remembered as follows:

- the *supra-aortic mediastinum*: from the thoracic inlet to the top of the aortic arch;
- the *subaortic mediastinum*: from the aortic arch to the superior aspect of the heart;
- the *paracardiac mediastinum*: from the heart to the diaphragm.

In each of these compartments, specific structures are consistently seen and need to be evaluated in every patient. The following description of normal anatomy is not comprehensive but is limited to the most important mediastinal structures.

Supra-Aortic Mediastinum

When one is evaluating a CT scan of this part of the mediastinum, it is a good idea to localize the *trachea* before doing anything else (Fig. 2.1A). The trachea is easy to recognize because it contains air, is seen in cross section, and has a reasonably consistent round or oval shape. It is relatively central in the mediastinum, from front to back and from right to left, and it serves as an excellent reference point. Many other mediastinal structures maintain a consistent relation to it.

At or near the thoracic inlet, the mediastinum is relatively narrow from front to back. The *esophagus* lies posterior to the trachea at this level (Fig. 2.1), but depending on the position of the trachea relative to the spine, the esophagus can be displaced to one side or the other, usually to the left. It is usually collapsed and appears as a flattened structure of soft-tissue attenuation, but small amounts of air or air and fluid are often seen in its lumen.

In the supra-aortic mediastinum, the great arterial branches of the aortic arch and the great veins are the most recognizable structures. At or near the thoracic inlet, the *brachiocephalic veins* are the most anterior and lateral vascular branches visible, lying immediately behind the clavicular heads (Fig. 2.1A and B). Although they differ in size, their positions are relatively constant. The great arterial branches (innominate, left carotid, and left subclavian arteries) are posterior to the veins and lie adjacent to the anterior and lateral walls of the trachea. They can be reliably identified by their relative positions, but variations are common.

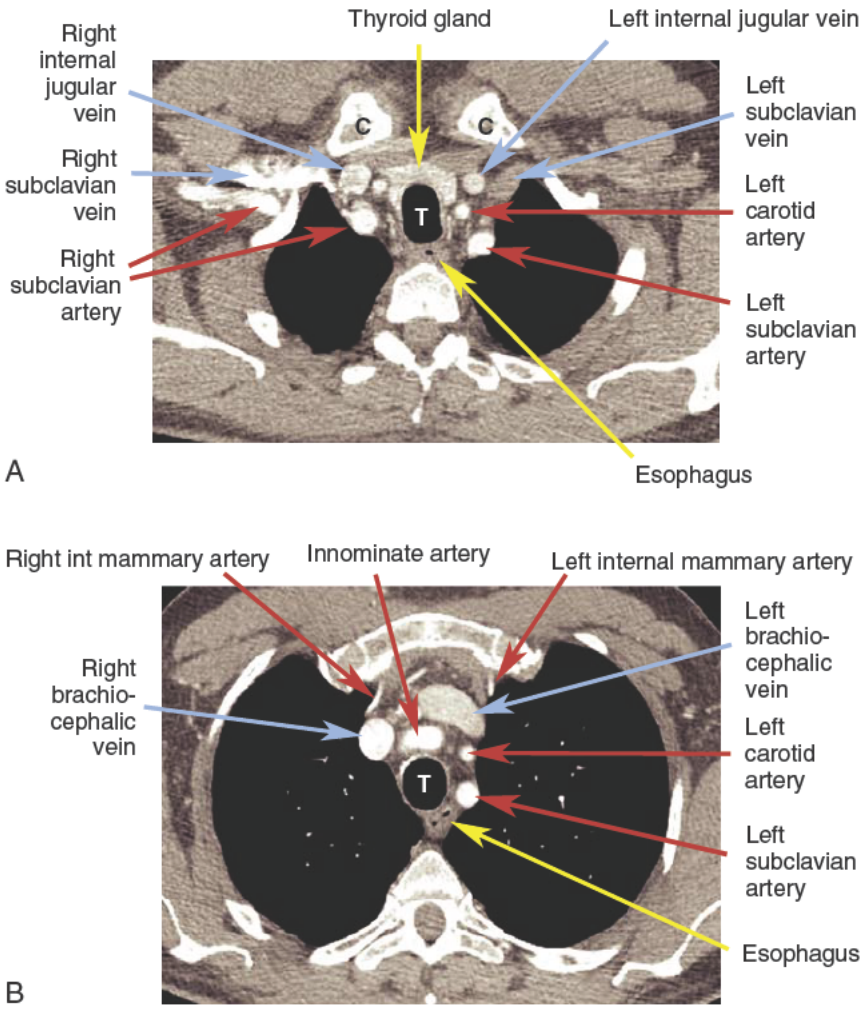

FIG. 2.1 Supra-aortic mediastinum. Contrast-enhanced CT with 1.25-mm slices. (A) Near the thoracic inlet, the trachea *(T)* is clearly seen, with the air-filled esophagus posterior and slightly to the left of it. The right and left subclavian and internal jugular veins are anterior and lateral and can be seen behind the clavicular heads *(C)* and clavicles. The great arterial branches (right carotid, right subclavian, left carotid, and left subclavian arteries) are visible on each side of the trachea. The thyroid gland is anterior and lateral to the trachea. Because of its iodine content, it appears denser than other soft tissue. (B) Just below (A) the brachiocephalic veins are visible anteriorly. The large arterial branches of the aorta lie posterior to the left brachiocephalic vein. The left subclavian artery is most posterior and is situated lateral to the left tracheal wall, at the three or four o'clock position relative to the tracheal lumen and contacting the mediastinal pleura. The left carotid artery is anterior to the left subclavian artery, at about the two o'clock position, and is somewhat variable in position. The innominate artery is usually anterior and slightly to the right of the tracheal midline. The internal *(int)* mammary arteries are visible bilaterally. (C) At a level below (B) the left *(Lt)* brachiocephalic vein is visible crossing the mediastinum from left to right. The subclavian, carotid, and innominate arteries maintain the same relative positions as in (B). The right *(Rt)* internal mammary *(mamm)* vein is visible arising from the right brachiocephalic vein. The densely opacified internal mammary *(int mamm)* arteries are visible bilaterally, lateral to the internal mammary veins. The esophagus contains a small amount of air in its lumen. (D) At a level below (C) the left brachiocephalic vein joins the right brachiocephalic vein, forming the superior vena cava. The major aortic branches are again clearly seen. The fat-filled pretracheal space is anterior to the trachea and posterior and medial to the arteries and veins. (E) The supra-aortic anatomy near the level of (D). The location of the pretracheal lymph nodes is shown, although these are not visible in (D). The location of the thymic remnant, although not seen well in (D), is also indicated. The approximate level of the scan in (D) is indicated by horizontal lines.

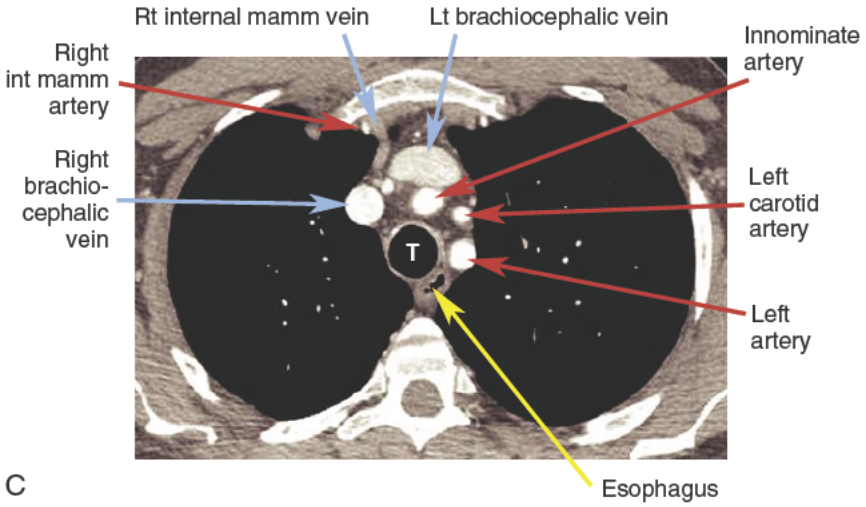

C

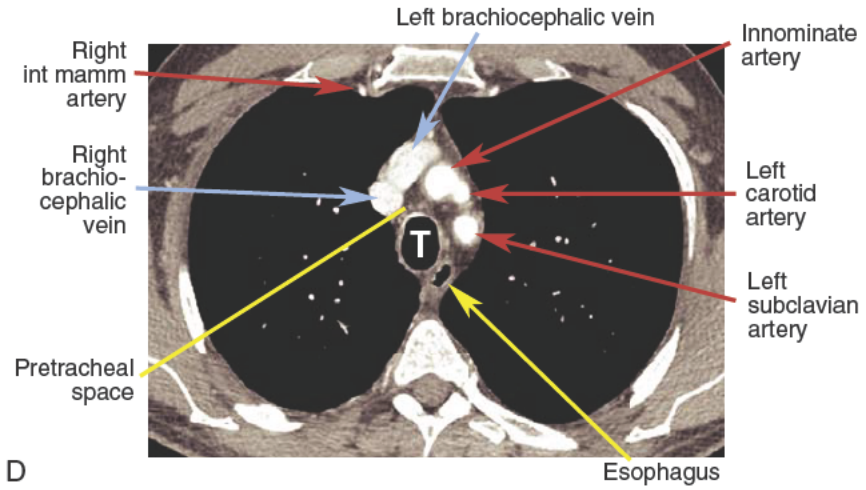

D

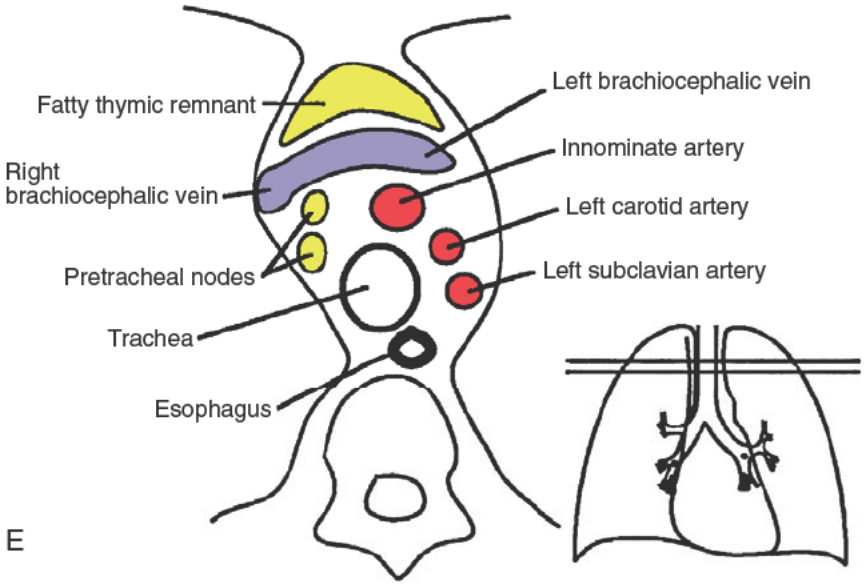

E

FIG. 2.1, cont'd

Below the thoracic inlet, anterior to the arterial branches of the aorta, the left brachiocephalic vein crosses the mediastinum from left to right (Fig. 2.1C) to join the right brachiocephalic vein, thus forming the *superior vena cava* (Fig. 2.1C–E). The *left subclavian artery* is most posterior and is situated adjacent to the left side of the trachea, at the three or four o'clock position relative to the tracheal lumen. The *left carotid artery* is anterior to the left subclavian artery, at the one or two o'clock position, and is somewhat variable in position. The *innominate artery* is usually anterior and somewhat to the right of the tracheal midline (11 or 12 o'clock position), but it is the most variable of all the great vessels and can have a number of different appearances in various patients or in the same patient at different levels.

Near its origin from the aortic arch, the innominate artery is usually oval and is somewhat larger than the other aortic branches. As it ascends toward the thoracic outlet, it may appear oval or elliptic because of its orientation or because of its bifurcation into the right subclavian and carotid arteries. This vessel can also be quite tortuous and can appear double if both limbs of a U-shaped part of the vessel are imaged in the same slice. Usually these vessels can be traced from their origin at the aortic arch to the point where they leave the chest, if there is any doubt as to what they represent.

Other than the great vessels, trachea, and esophagus, little is usually seen in the supra-aortic mediastinum. A few lymph nodes are normally visible. Small vascular branches, particularly the *internal mammary veins*, can be seen in this part of the mediastinum. In some patients the *thyroid gland* may extend into this portion of the mediastinum, and the right and left thyroid lobes may be visible on each side of the trachea. This appearance is not abnormal and does not imply thyroid enlargement. On CT the thyroid can be distinguished from other tissues or masses because its attenuation is greater than that of soft tissue (because of its iodine content). The *thymus* is sometime visible at this level anterior to the large vessels described earlier, within the *prevascular space* (described further later).

Subaortic Mediastinum

The subaortic mediastinum extends inferiorly from the top of the aortic arch to the upper portion of the heart (Fig. 2.2). Whereas the supra-aortic region largely contains arterial and venous branches of the aorta and vena cava, this compartment contains many of the undivided mediastinal great vessels (the aorta, superior vena cava, and pulmonary arteries). This compartment also contains most of the important mediastinal lymph node groups. A few key levels in this part of the mediastinum will be discussed in detail.

Aortic Arch Level

In the upper portion of the subaortic mediastinum, the *aortic arch* is easily seen and has a characteristic but somewhat variable appearance (Fig. 2.2A). The aortic arch is seen anterior and to the left of the trachea, with the posterior arch lying anterior and lateral to the spine. Usually the aortic arch is about the same diameter in its anterior and mid portions, although the posterior arch is typically somewhat smaller. The position of the anterior and posterior aspects of the arch can vary in the presence of atherosclerosis and aortic tortuosity; in patients with a tortuous aorta, the anterior arch is displaced to the right, whereas the posterior aortic arch is displaced laterally and posteriorly, to a position to the left of the spine.

At this level the *superior vena cava* is visible anterior and to the right of the trachea and is usually oval (Fig. 2.2A–C). The *esophagus* appears the same as at higher levels and is variable in position. It is posterior to the trachea and often lies to the left of the tracheal midline.

A somewhat triangular region, with the apex of the triangle directed anteriorly, marginated by the aortic arch on the left, the superior vena cava and mediastinal pleura on the right, and the trachea posteriorly, represents the *pretracheal* or *anterior paratracheal* space (Fig. 2.2A and C). This fat-filled space is important because it contains middle mediastinal lymph nodes in the paratracheal chain, which are commonly involved in various lymph node diseases. Whenever the mediastinum is being viewed for diagnosis of lymphadenopathy, you should look here first. Other mediastinal node groups are closely related pretracheal nodes, both spatially and in regard to lymphatic drainage. It is not uncommon to see a few normal-sized lymph nodes (short-axis or least diameter less than 1 cm) in the pretracheal space (see the review of mediastinal lymphadenopathy in Chapter 4 for a detailed discussion of this topic).

Anterior to the great vessels (aorta and superior vena cava) is another roughly triangular space called the *prevascular space* (Fig. 2.2A–C). This compartment constitutes part of the anterior mediastinum and primarily contains the thymus, lymph nodes, and fat. The apex of this triangular space represents the anterior junction line, which is sometimes visible on chest radiographs.

In young patients (generally up to 30 years of age), CT shows the *thymus* to be of soft-tissue attenuation and bilobed or arrowhead shaped, with each of the

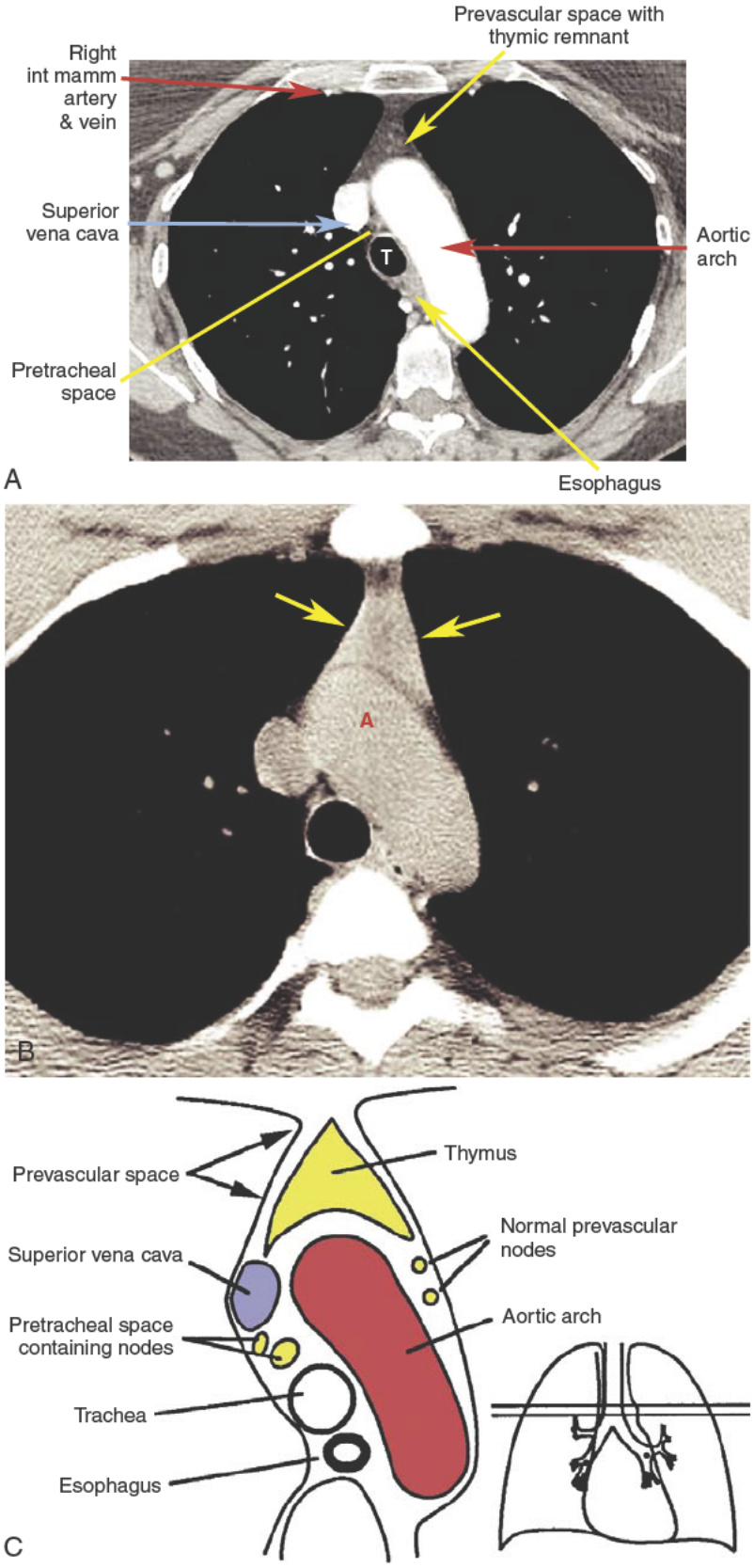

FIG. 2.2 Subaortic mediastinum. Contrast-enhanced CT with 1.25-mm slices. At the aortic arch level, (A) the aortic arch extends from a position anterior to the trachea *(T)* to the left, with the posterior part of the arch usually lying anterior and lateral to the spine. The superior vena cava contacts the right mediastinal pleura and together with the aortic arch delineates the pretracheal space. The prevascular space is anterior to the great vessels and contains the thymus, which is largely replaced by fat in this patient. (B) In a 21-year-old patient a large normal thymus with soft-tissue attenuation *(arrows)* occupies most of the prevascular space. It is separated from the aortic arch *(A)* by a fat plane. (C) The mediastinal anatomy at the aortic arch level.

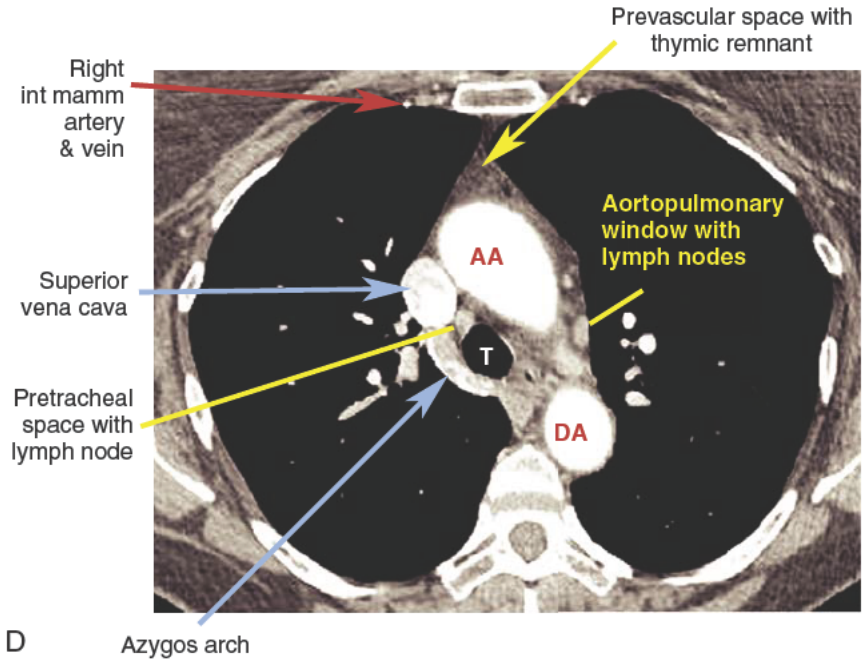

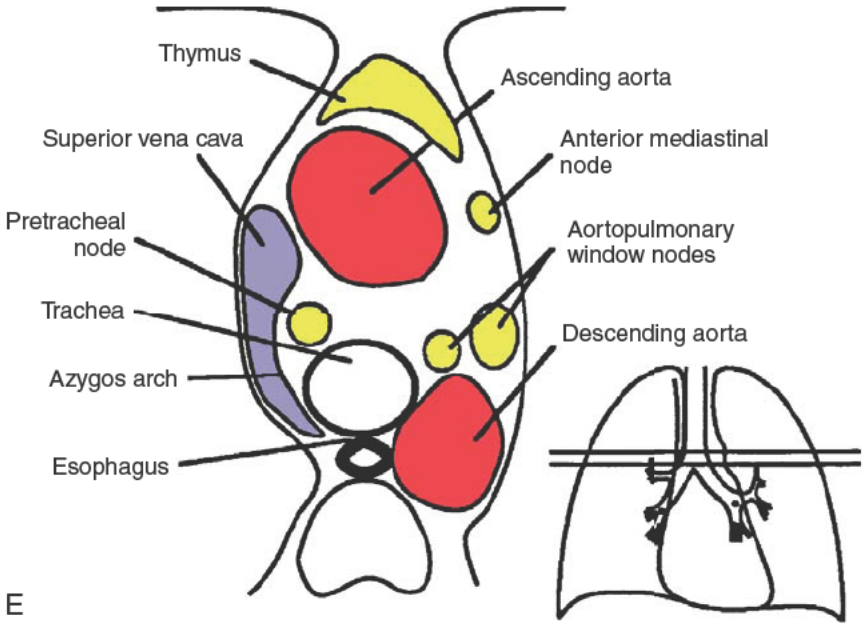

FIG. 2.2, cont'd At the azygos arch and aortopulmonary window level, (D) the azygos arch is usually visible arising from the posterior aspect of the superior vena cava, contacting the right mediastinal pleura, and forming the lateral margin of the node bearing pretracheal space. Fat visible under the aortic arch but above the pulmonary artery is in the aortopulmonary window, which also contains lymph nodes. (E) The mediastinal anatomy at the azygos arch and aortopulmonary window level.

two lobes (right and left) contacting the mediastinal pleura and occupying most of the prevascular space. Each lobe is usually 1 to 2 cm thick (measured perpendicular to the pleura), but this differs (Fig. 2.2B). In later adulthood the thymus involutes, with soft tissue being replaced by fat. In patients older than 30 years the prevascular space appears fat filled, with thin wisps of tissue passing through the fat. Most of this, including the fat, represents the thymus. At higher levels the thymus is sometimes visible anterior to the brachiocephalic arteries and veins, also within the prevascular space.

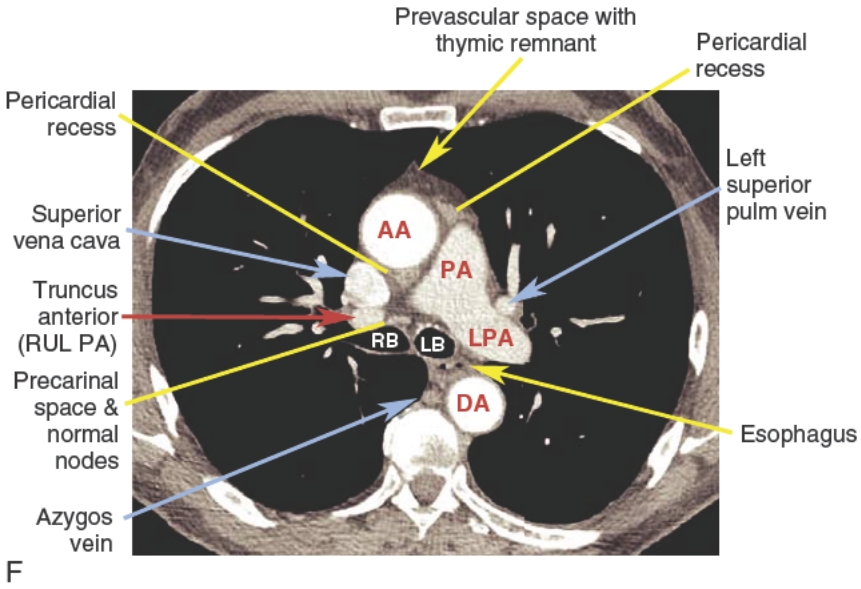

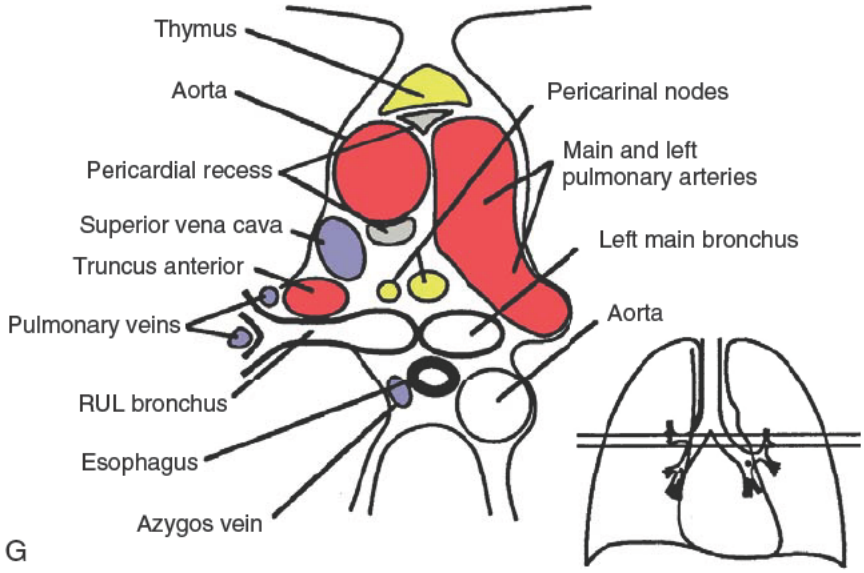

FIG. 2.2, cont'd At the main pulmonary artery, subcarinal space, and azygoesophageal recess level, (F) at the tracheal carina, the right main bronchus *(RB)* and left main bronchus *(LB)* are visible as separate branches. The main pulmonary artery *(PA)* is contiguous with the left pulmonary artery *(LPA)* more posteriorly. The truncus anterior (pulmonary artery supplying most of the right upper lobe, *RUL*) is visible as an oval structure anterior to the right main bronchus. Normal pericardial recesses containing fluid are visible posterior to the ascending aorta *(AA)* and between the anterior aorta and the main pulmonary artery. These are relatively low in attenuation and should not be confused with abnormal lymph nodes. The precarinal space containing lymph nodes is contiguous with the pretracheal space. (G) The mediastinal anatomy at this level.

Continued

Azygos Arch and Aortopulmonary Window Level

At a level slightly below the aortic arch, the ascending aorta and descending aorta are visible as separate structures. Characteristically the ascending aorta (25–35 mm in diameter) is slightly larger than the descending aorta (20–30 mm).

On the right side, the arch of the *azygos vein* (*azygos* means *unpaired*) arises from the posterior wall of the superior vena cava, passes over the right main bronchus (thus it is seen at a higher level than the bronchus itself), and continues posteriorly along the mediastinum, to lie to the right of and anterior to the spine (Fig. 2.2D and E). Below the level of the azygos arch,

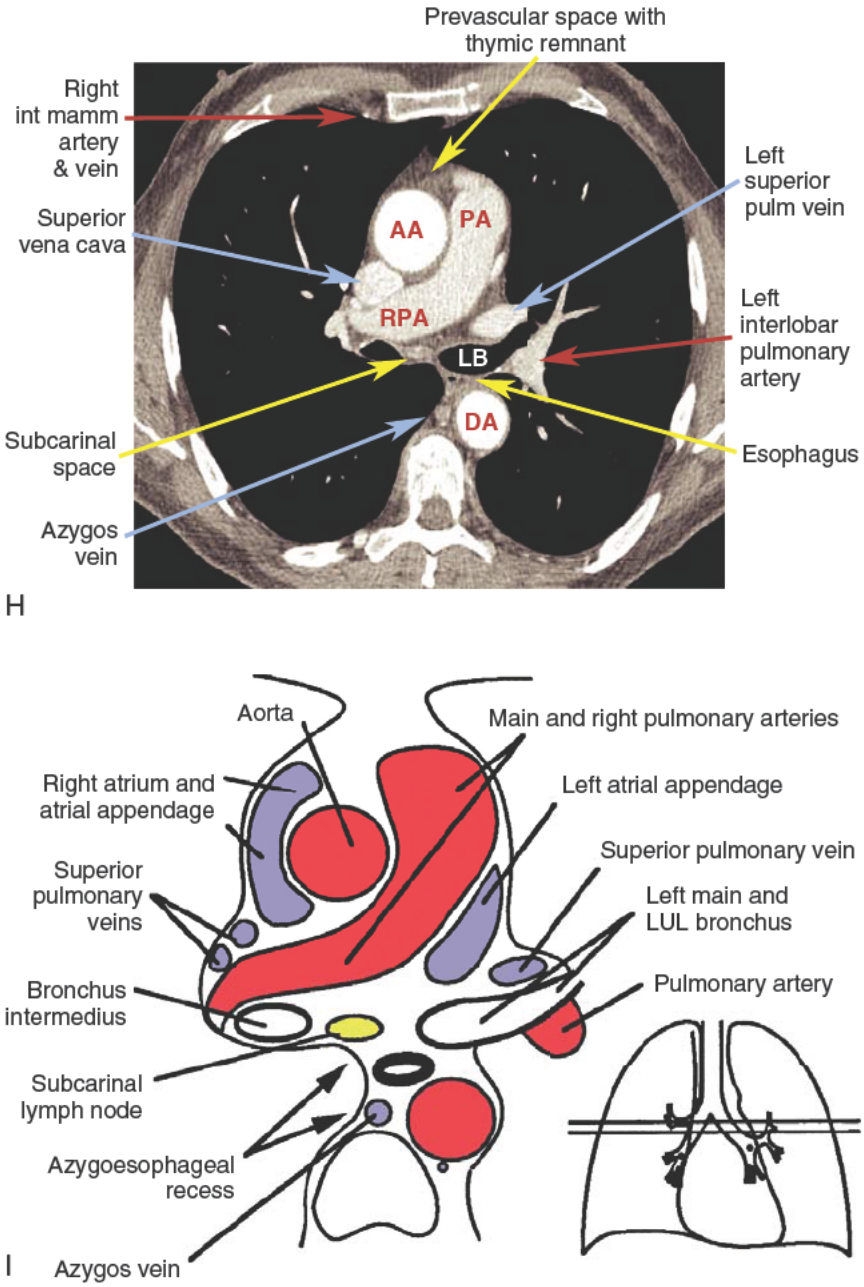

FIG. 2.2, cont'd (H) Scan and (I) diagram below the tracheal carina, at the level of the right pulmonary artery and azygoesophageal recess. The right pulmonary artery *(RPA)* is visible crossing the mediastinum, filling the pretracheal and precarinal space. A small amount of fat and a normal lymph node are visible in the subcarinal space, slightly anterior to the esophagus, azygos vein, and azygoesophageal recess. The recess appears concave laterally, with the mediastinal pleura closely related to the azygos vein and esophagus. *AA*, Ascending aorta; *DA*, descending aorta; *int mamm*, internal mammary; *LB*, left bronchus; *LUL*, left upper lobe; *PA*, pulmonary artery; *pulm*, pulmonary; *RUL*, right upper lobe; *T*, trachea.

the azygos vein remains visible in this position. The azygos arch is often visible on one or two adjacent slices and sometimes appears nodular. However, its characteristic location is usually sufficient to correctly identify this structure. When the azygos arch is visible, it marginates the right border of the pretracheal space.

On the left side of the mediastinum, under the aortic arch but above the main pulmonary artery, is the region termed the *aortopulmonary* (or *aorticopulmonary*) *window*. The aortopulmonary window contains fat, lymph nodes (middle mediastinal), the recurrent laryngeal nerve, and the ligamentum arteriosum

(the latter two are usually invisible, although a calcified ligamentum is sometimes seen; Fig. 2.2D and E). *Aortopulmonary window lymph nodes* freely communicate with those in the pretracheal space, and it may be difficult to distinguish nodes in the medial aortopulmonary window from those in the left part of the pretracheal space. In some patients the aortopulmonary window is not clearly visible, with the main pulmonary artery lying immediately below the aortic arch. In such patients it is difficult to distinguish lymph nodes from volume averaging of the adjacent aorta and pulmonary artery, unless thin slices are obtained.

Main Pulmonary Arteries, Subcarinal Space, and Azygoesophageal Recess Level

At or slightly below the aortopulmonary window, at the level the *ascending aorta* is first seen in cross section (i.e., it is round or nearly round), a portion of the pericardium, usually containing a small amount of pericardial fluid, extends up from below into the pretracheal space, lying immediately behind the ascending aorta. This is termed the *superior pericardial recess* (Fig. 2.2F and G). Although it can sometimes be confused with a lymph node, its typical location, immediately behind and hugging the aortic wall, its oval or crescentic shape, and its relatively low (water) attenuation allow it to be distinguished from a significant abnormality. Another part of the pericardial recess can sometimes be seen anterior to the ascending aorta and pulmonary artery (Fig. 2.2F and G).

At or near this level the trachea bifurcates into the right and left main bronchi. The *carina* itself is usually visible on CT (Fig. 2.2F).

Below the level of the carina and azygos arch (Fig. 2.2F–I), the medial aspect of the right lung tucks into the posterior portion of the middle mediastinum, adjacent to the azygos vein and esophagus. This part of the mediastinum, reasonably termed the *azygoesophageal recess*, is important because of its close relationship to the esophagus, the main bronchi, and the subcarinal space containing lymph nodes. The azygoesophageal recess appears concave laterally in most normal individuals. A convexity in this region may be attributed to the esophagus, azygos vein, enlarged lymph nodes, or a mass.

In many people, the azygoesophageal recess is somewhat posterior to the node-bearing *subcarinal space*, which lies between the main bronchi. Normal nodes are commonly visible in this space, because they are larger than normal nodes in other parts of the mediastinum and up to 1.5 cm in short-axis diameter. The esophagus is usually seen immediately behind the subcarinal space, and distinguishing nodes and the esophagus may be difficult unless the esophagus contains air or contrast material, or its course can be traced on adjacent slices. At levels below the subcarinal space, the appearance of the azygoesophageal recess is relatively constant, although it narrows in the retrocardiac region.

Also at or near this level the *main pulmonary artery* divides into its right and left branches. The *left pulmonary artery* (Fig. 2.2F–I) is somewhat higher than the right, usually seen 1 cm above it, and appears to be the continuation of the main pulmonary artery, directed posterolaterally and to the left. The *right pulmonary artery* arises at an angle of nearly 90 degrees to the main and left pulmonary arteries and crosses the mediastinum, anterior to the carina or the main bronchi. In this location the right pulmonary artery effectively fills in the pretracheal space. At the point the main bronchi and pulmonary arteries exit the mediastinum, the pulmonary hila are visible (see Chapter 5).

Paracardiac Mediastinum

On progression caudally through the mediastinum, the origins of the great vessels from the cardiac chambers can be seen to a variable degree. Although CT is not commonly used to diagnose cardiac abnormalities (echocardiography or magnetic resonance imaging is usually preferred), a simple understanding of cardiac anatomy on CT can be helpful in diagnosis, and its use is increasing with gated multidetector techniques.

The *main pulmonary artery* or pulmonary outflow tract is most anterior and is continuous with the right ventricle, which can be seen at lower levels as anterior and to the right of the ascending aorta or left ventricle (Fig. 2-3A–C). The superior vena cava joins the right atrium, which is elliptic or crescentic. The *right atrial appendage* extends anteriorly from the upper atrium, bordering the right mediastinal pleura.

Between the right atrium and the main pulmonary artery or pulmonary outflow tract, the *aortic root* enters the left ventricle. At this level it is common in adults to see some coronary artery calcification (Fig. 2.3A–C), and often, uncalcified *coronary arteries* (left main coronary artery, left anterior descending coronary artery, circumflex coronary artery, and right coronary artery) are visible surrounded by mediastinal fat. Coronary artery anatomy is discussed further in Chapter 3.

The *left atrium* is posteriorly located, usually appearing larger than the right. The *left atrial appendage* extends anteriorly and to the left and is visible below the left pulmonary artery, bordering the pleura. On each side the *superior and inferior pulmonary veins* can be seen entering the left atrium (Fig. 2.3A–E; see Chapter 5 for further discussion).

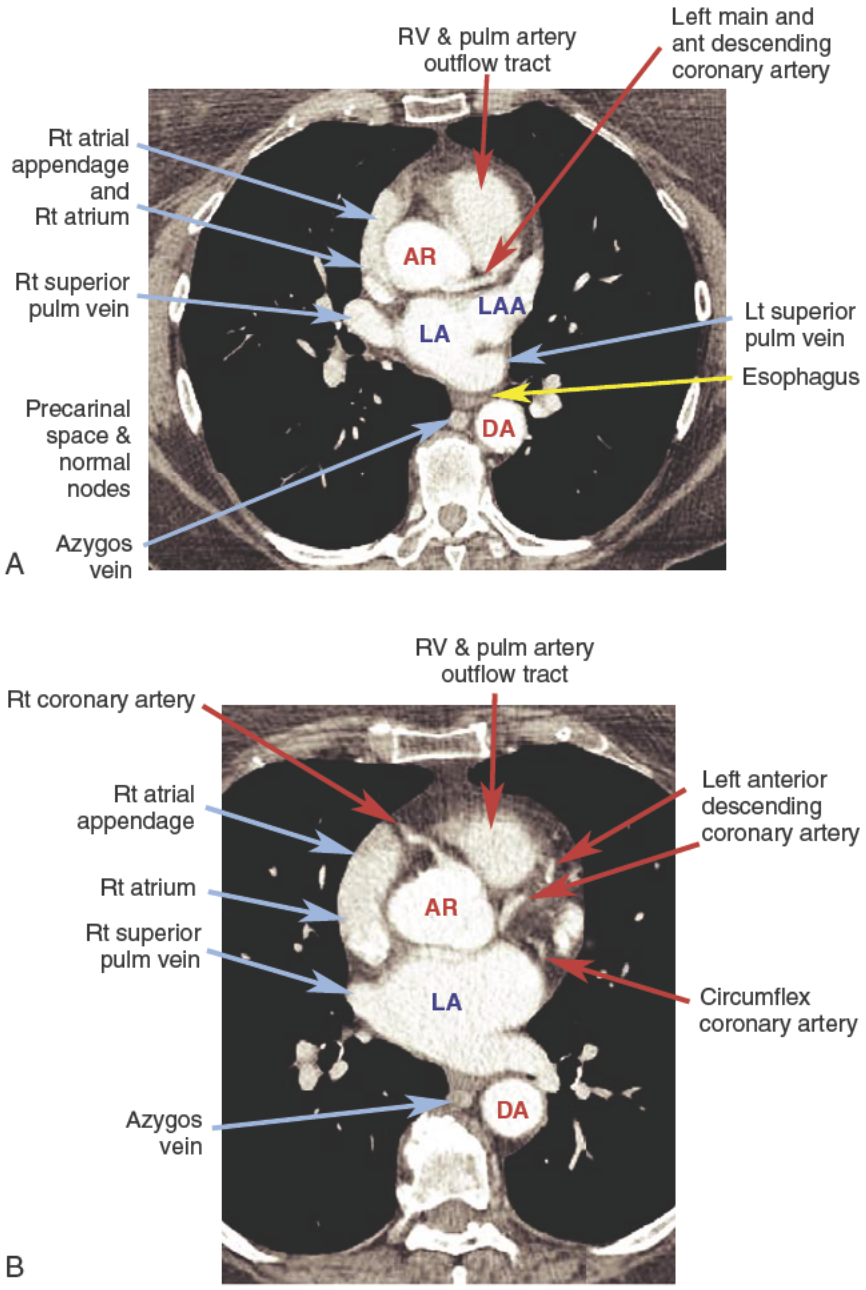

FIG. 2.3 Paracardiac mediastinum. Contrast-enhanced 1.25-mm-slice spiral CT. (A) Most cephalad, the origins of the aorta and pulmonary artery are visible, with the aortic root *(AR)* in a central position. The right ventricular *(RV)* or pulmonary *(pulm)* outflow tract or main pulmonary artery is anterior and to the left of the aortic root at this level. The right atrium, with its appendage extending anteriorly, borders the right mediastinal pleura. The superior pulmonary veins usually enter the upper aspect of the left atrium *(LA)* at this level. The left atrial appendage *(LAA)* is also seen. The origin of the left main coronary artery (which is short) is visible at this level and is continuous with the anterior *(ant)* descending coronary artery. (B) A slice slightly below (A) showing the origin of the right coronary artery and the left anterior descending and circumflex branches of the left coronary artery.

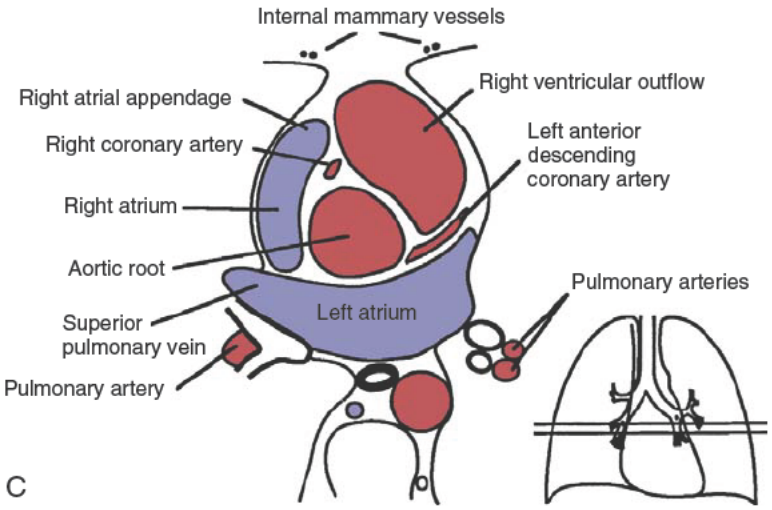

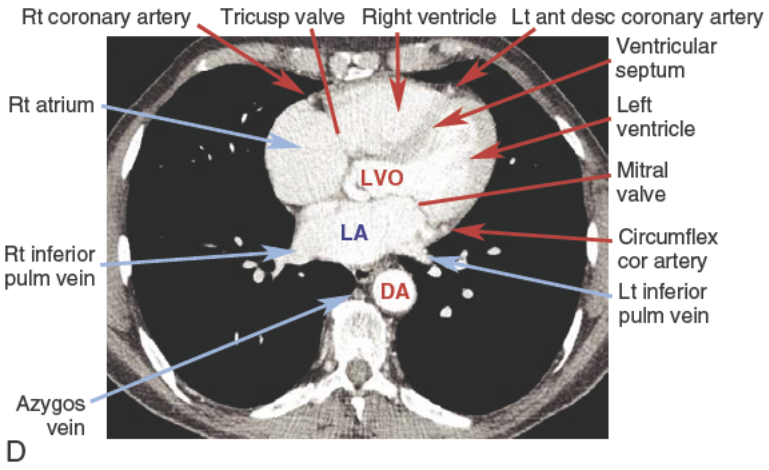

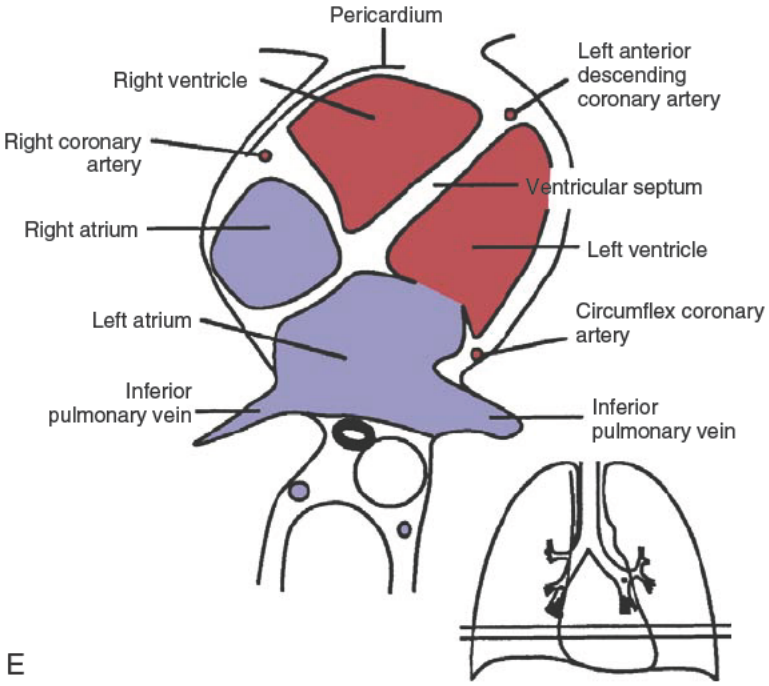

FIG. 2.3, cont'd (C) Diagram at the levels of (A) and (B). (D and E) At a lower level the right atrium, left atrium *(LA)*, and right and left ventricles are visible. The right ventricle is located anterior and to the right of the left ventricle. The ventricular septum and left ventricular walls are thicker than the right ventricular wall. The locations of the tricuspid *(tricusp)* and mitral valves can be identified. The left ventricular outflow *(LVO)* is visible on the scan.

Continued

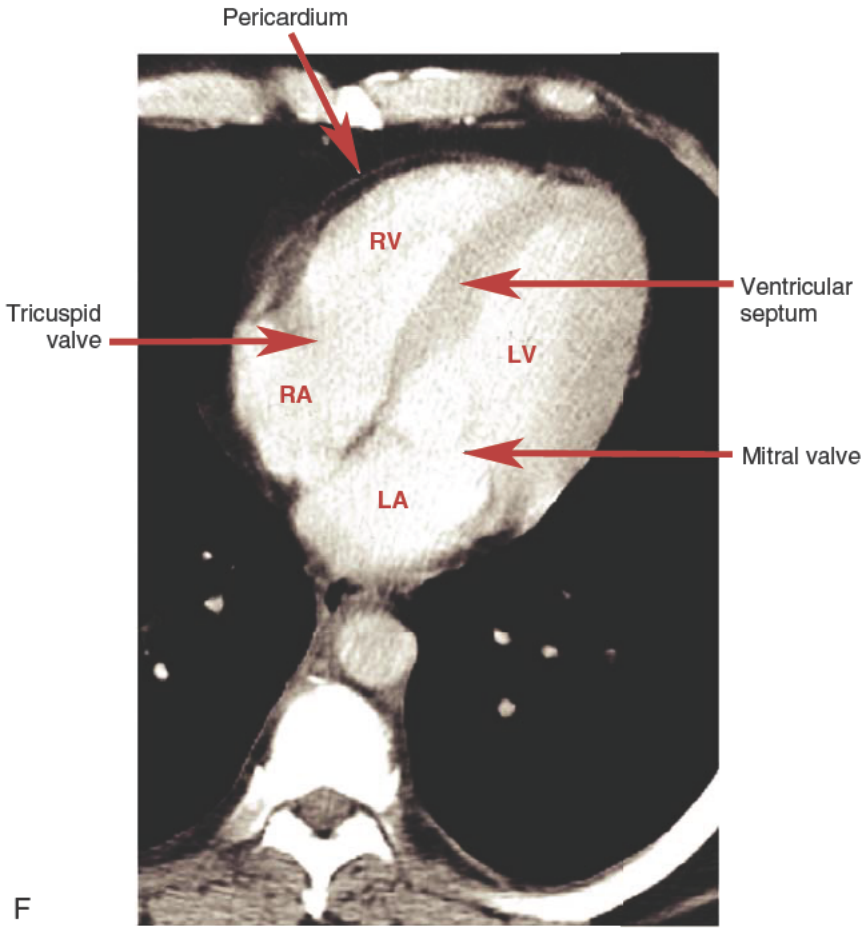

F

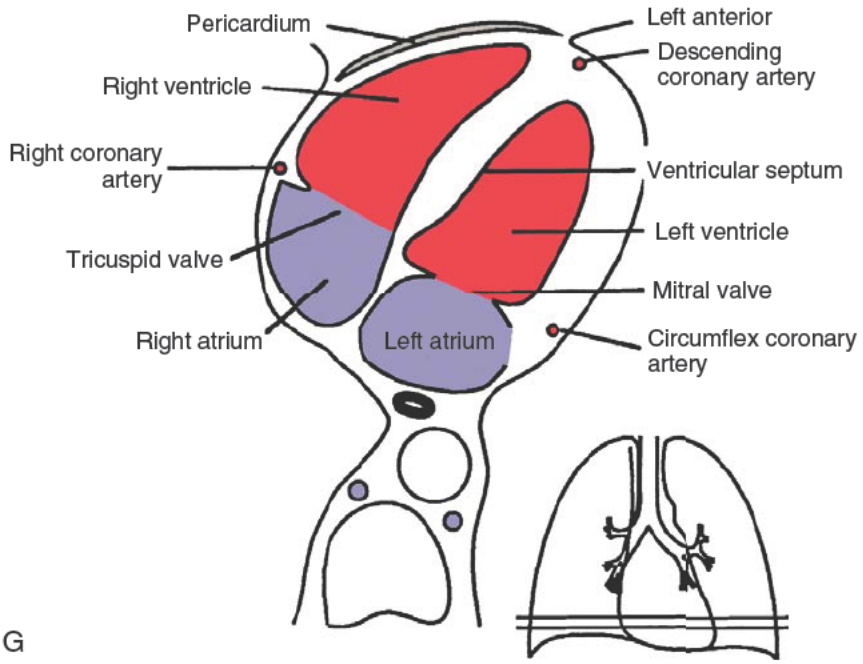

G

FIG. 2.3, cont'd (F and G) All four chambers are visible at this level, and the locations of the tricuspid and mitral valves can be identified. The interventricular septum and free wall of the left ventricle *(LV)* are considerably thicker than the wall of the right ventricle *(RV)*. The pericardium is visible as a thin white line surrounded by mediastinal fat. It should appear to be 1 to 2 mm thick.